Supplemental Materials

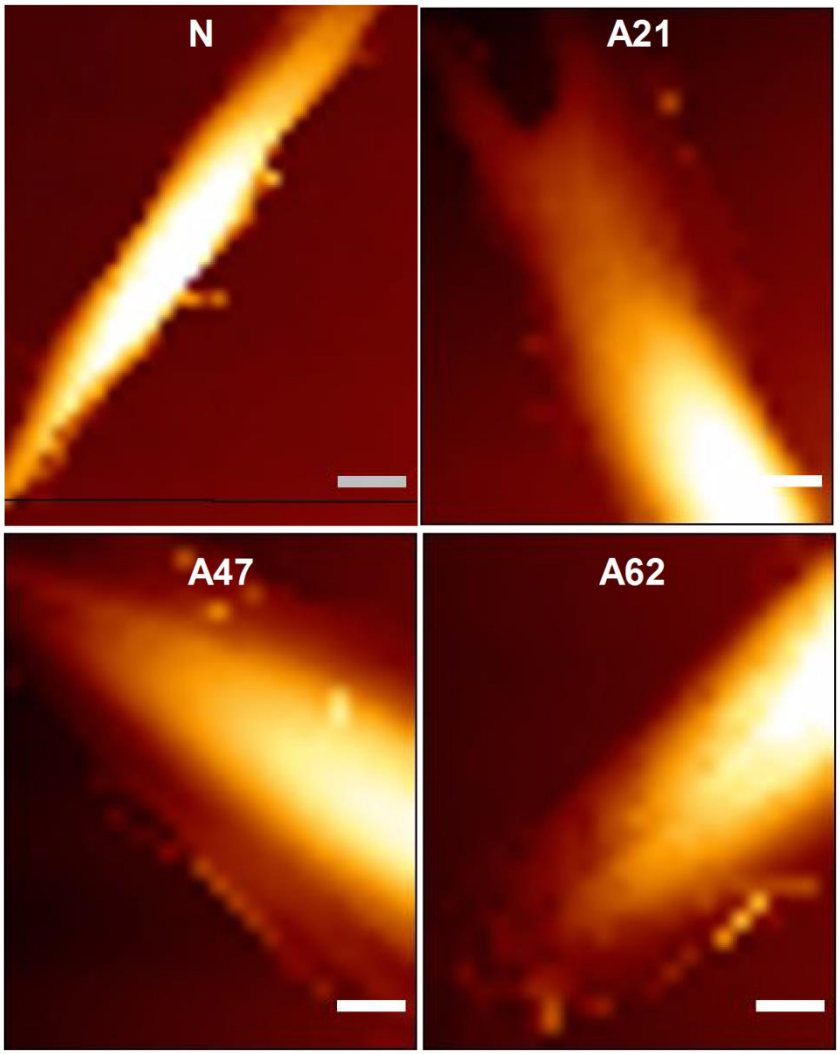

Figure S1. AFM topography images of cells from different donors**.** Representative topography images indicate that cell area is increased for cells from adult donors. Scale bars represent 10 μm.

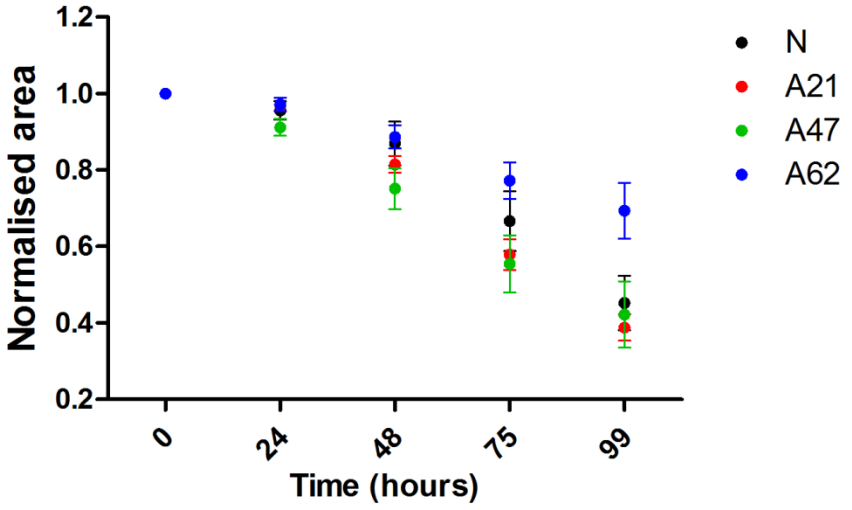

Figure S2. Donor ageing reduces cell migration of cell monolayer. Migration of fibroblast cells at different donor ages was assessed based on a wound healing assay. To evaluate the rate of cell migration, the area of gap was calculated at each time point and normalised to the initial area. Cells from oldest donor exhibit decreased migration compared to cells from other donors.

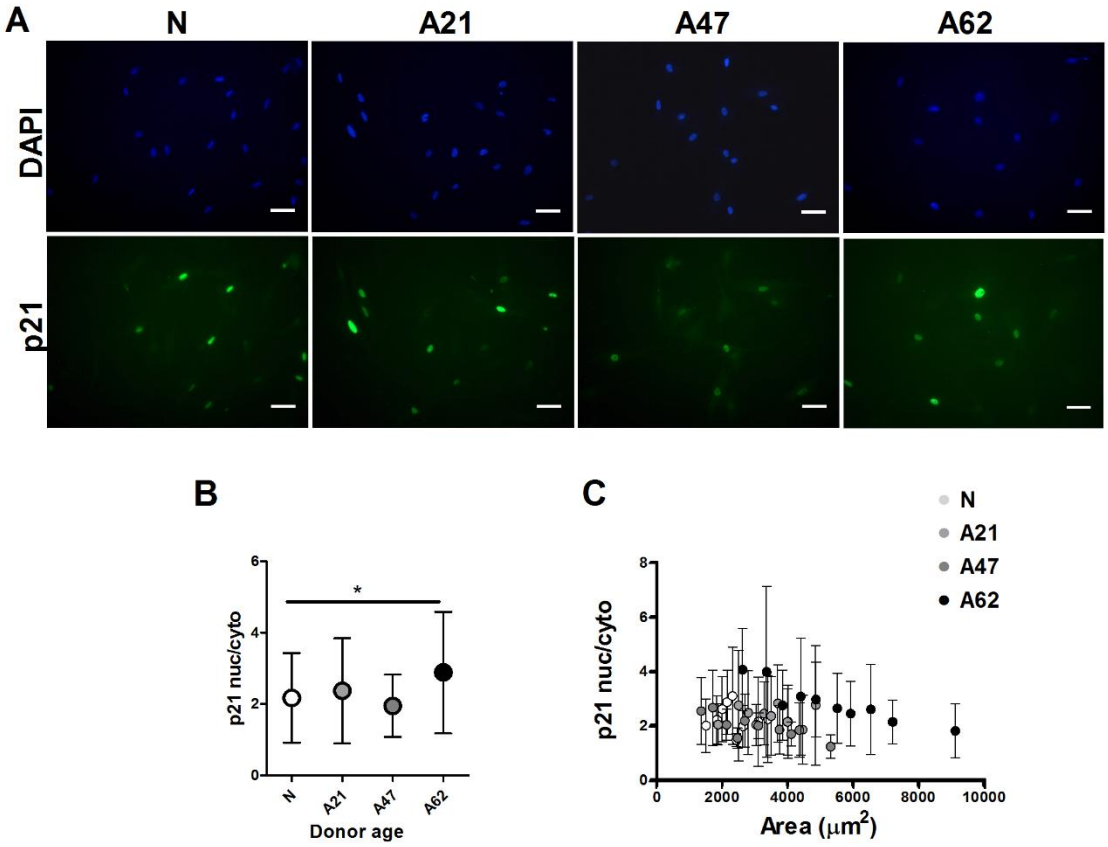

Figure S3. Correlation between p21 cell senescence marker and donor ageing. (A) Representative epifluorescence images of p21 localisation in cells from neonatal and adult donors. Cells are labelled,

nucleus DAPI (blue), p21 (green). Scale bars represent 50 μm. (B) Immunostaining analysis showing a significant increase of p21 in cells from oldest donor. (C) Corresponding plot showing correlation between p21 localisation to cell area. Independantly to donor age, there is no a significant correlation between p21 localisation and cell area. Data is presented as mean values with SD (nonparametric one way ANOVA test, * $p<0.05$).

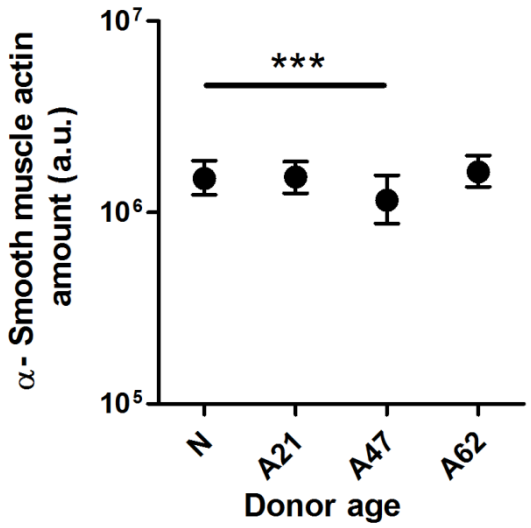

Figure S4. Expression of alpha- smooth muscle actin in cells from different donors. There was no a significant trend of expression of alpha- smooth muscle actin and donor age. Only significant reduction was seen compare cells from neonatal donor to cells from adult donor at 47 year age. . Data is presented as geometric mean with quartiles (nonparametric one way ANOVA test, *** $p<0.001$).

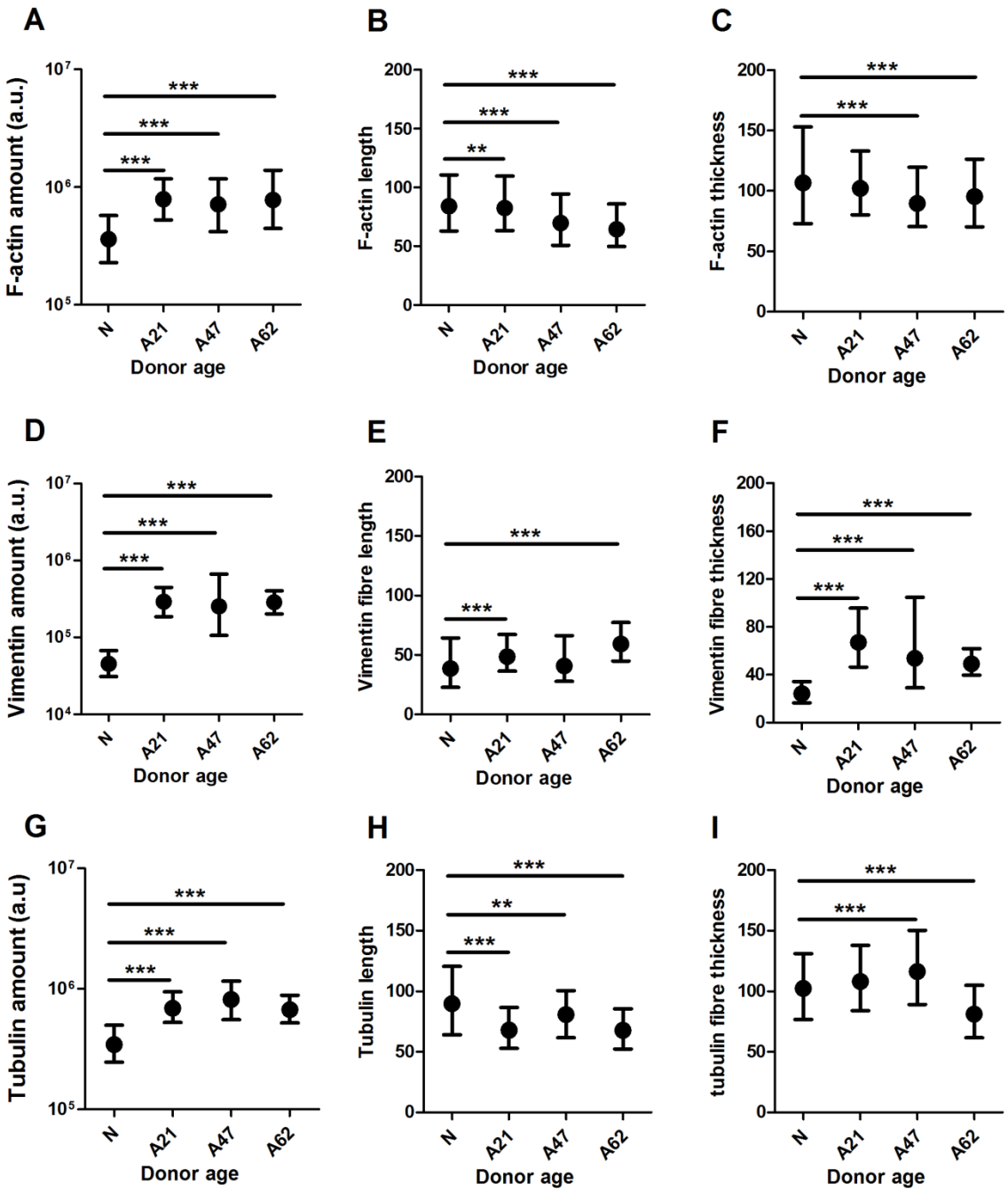

Figure S5. Cells from aged donors exhibited changes in the main three cytoskeletons. F-actin cytoskeleton showing a significant increase in (A) fibre amount and reduction in (B) fibre length and (C) fibre thickness for cells from aged donors. Intermediated filament vimentin (D) fibre amount, (E) fibre length and (F) fibre thickness significantly incresed in cells from aged donors compared to cells from neonatal donor. (G-I) Corresponding plots of microtubules showing significant changes in cells from aged donors. (** $p<0.01$, *** $p<0.001$, Mann Whitney U test). Data plotted from three independent experiments and presented as geometric mean with quartiles. Cell number varies between (280-620).

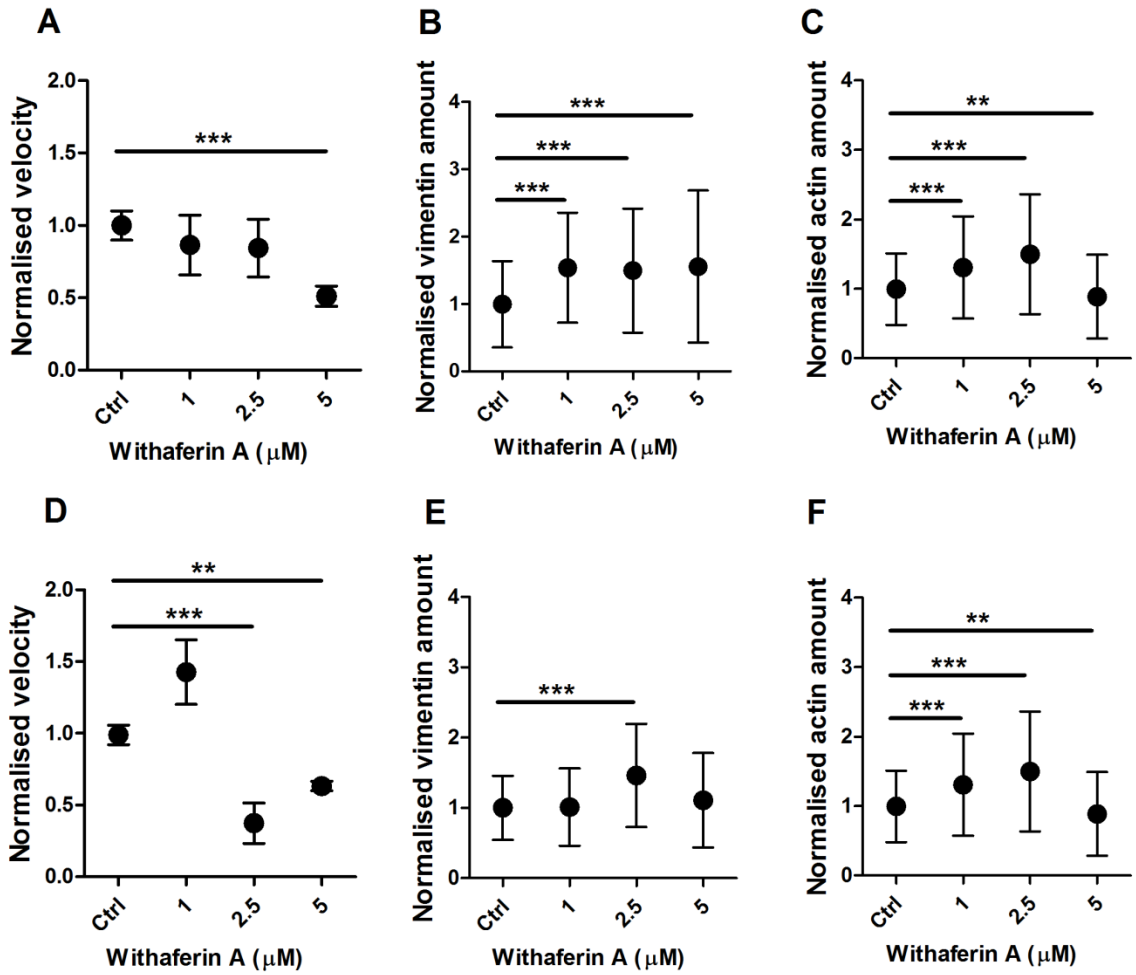

Figure S6. Withaferin A treatment reduced cell migration independantly to donor age. Fibroblast cells from neonatal donor exhibided reduction in (A) cell velocity, which was correlated with increased (B) vimentin and (C) actin amount after drug treatment. Data is plotted from at least three independent experiment and normalised to control conditions. Plots are presented as mean with SD (paired t-test, * $p<0.05$ ** $p<0.01$, *** $p<0.001$). Cell number for velocity measurement range between (18-20). Vimentin and actin amount (263-311). Fibrobast cells from adult donor at age 47 year showing reduction in (D) cell velosity with slight increase of (E) vimentin amount and decrease in (F) actin amount. Data is plotted from at least three independent experiment and normalised to control canditions. Plots are presented as a mean with SD (paired t-test, * $p<0.05$ ** $p<0.01$, *** $p<0.001$). Cell number for velocity measurement range between (22-36). Vimentin and actin amount (126-146).

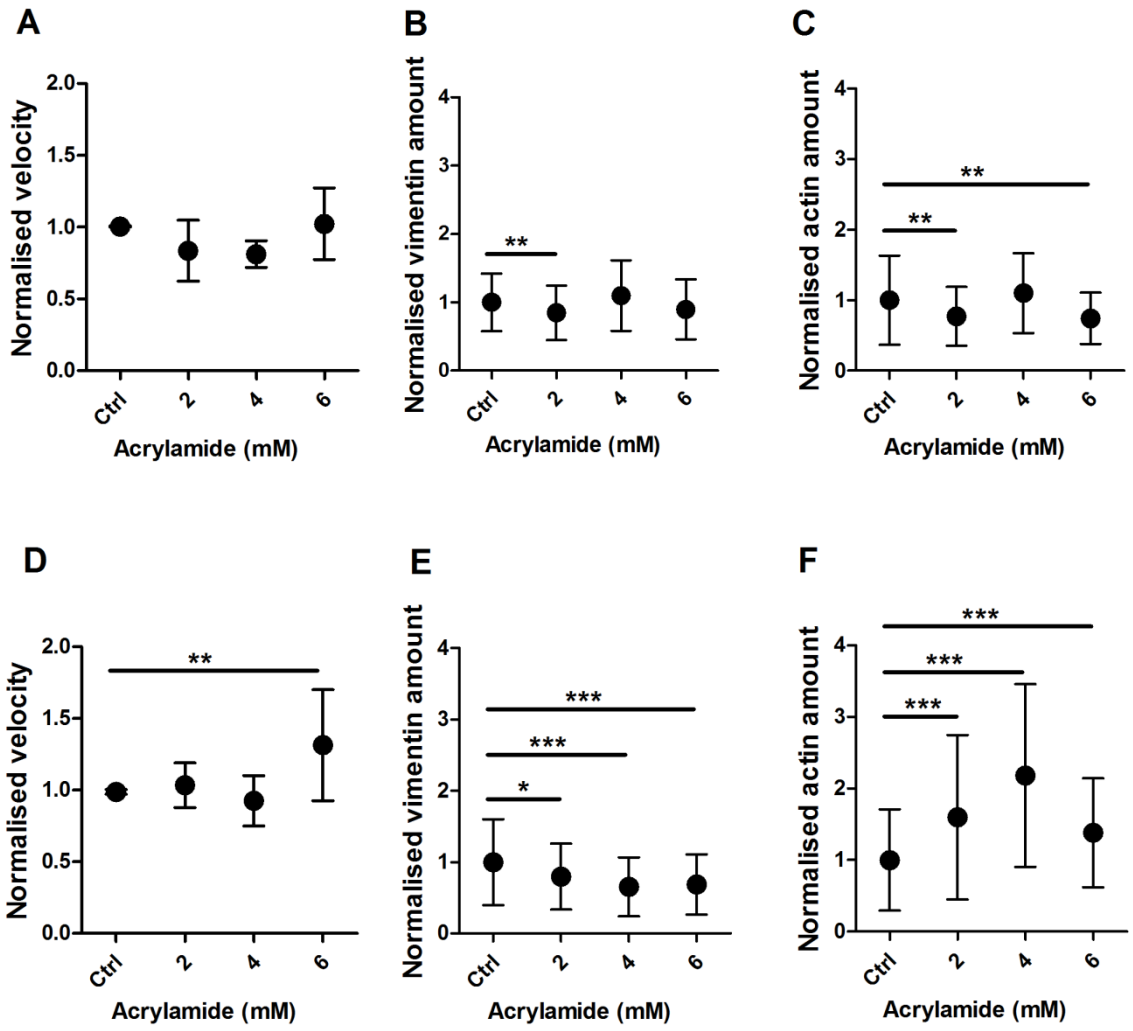

Figure S7. Acrylamide treatment has a higher effect on cell migration for cells from aged donor. Fibroblast cells from neonatal donor showing no effect on (A) cell migration in response to acrylamide treatment. Corresponding plots indicate no changes in (B) vimentin amount and reduction in (C) actin amount. Data is plotted from at least three independent experiment and normalised to control canditions. Plots are presented as a mean with SD (paired t-test, * $p<0.05$ ** $p<0.01$, *** $p<0.001$). Cell number for velocity measurement range between (26-34), vimentin and actin amount (138-170). Fibroblast cells from adult donor at age 47 years showing increase (D) cell velosity. Corresponding plots showing a significant reduction in (E) vimentin amount and significant increse in (F) actin amount. Data is plotted from at least three independent experiment and normalised to control canditions. Plots are presented as a mean with SD (paired t-test, * $p<0.05$ ** $p<0.01$, *** $p<0.001$). Cell number for velocity measurement range between (26-33), vimentin and actin amount (117-170).

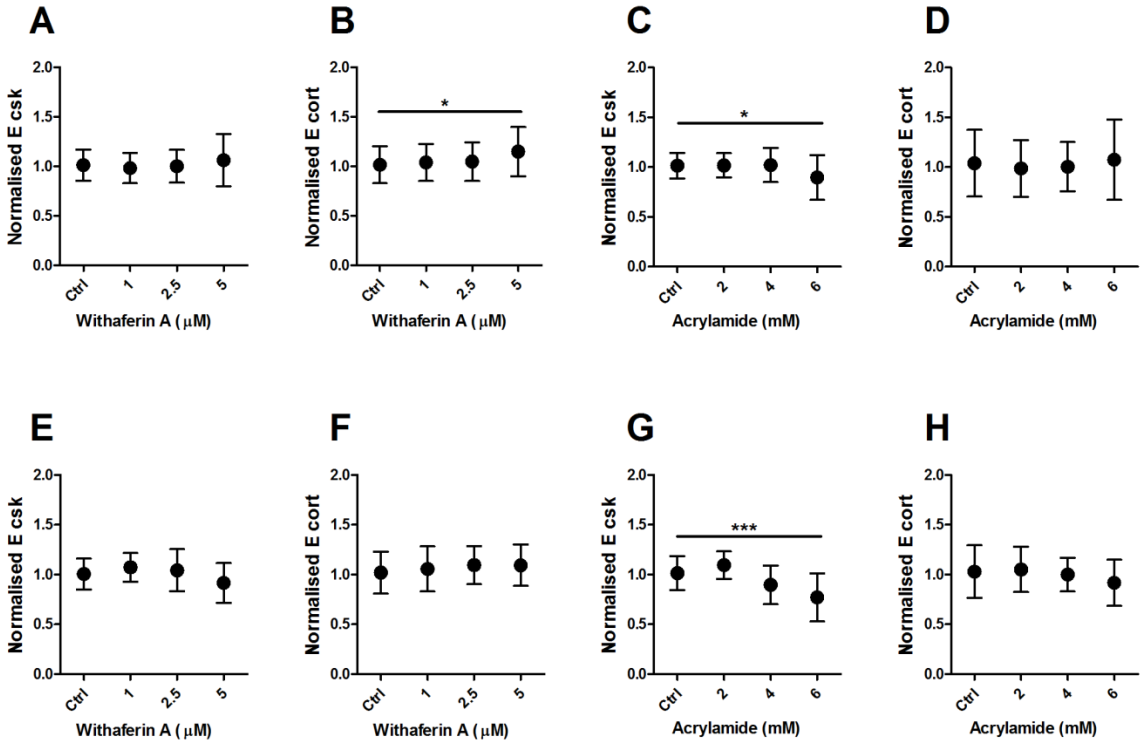

Figure S8. Fibroblast cells from neonatal donor treated with withaferin A show increase in (A) cell cytoskeleton Young's modulus, and in (B) cortical Young's modulus, but treated with acryamide show reduction in (C) cytoskeleton Young's modulus and no changes in (D) cortical Young's modulus. Data is plotted from at least three independent experiment and normalised to control conditions. Plots are presented as a mean with SD (paired t-test, * $p<0.05$). Cell number range for withaferin A (26-48) and acrylamide (39-67). Cells from adult donor treated with withaferin A exhibited no changes in cell (E) cytoskeleton Young's modulus and (F) cortical Young;s modulus, but show a reduction in (G) cytoskelon Young's modulus and no effect to (H) cortical Young's modulus after treatment with acrylamide. Data is plotted from at least three independent experiment and normalised to control conditions. Plots are presented as a mean with SD (paired t-test, *** $p<0.001$). Cell number range for withaferin A (26-55) and acrylamide (28-57).

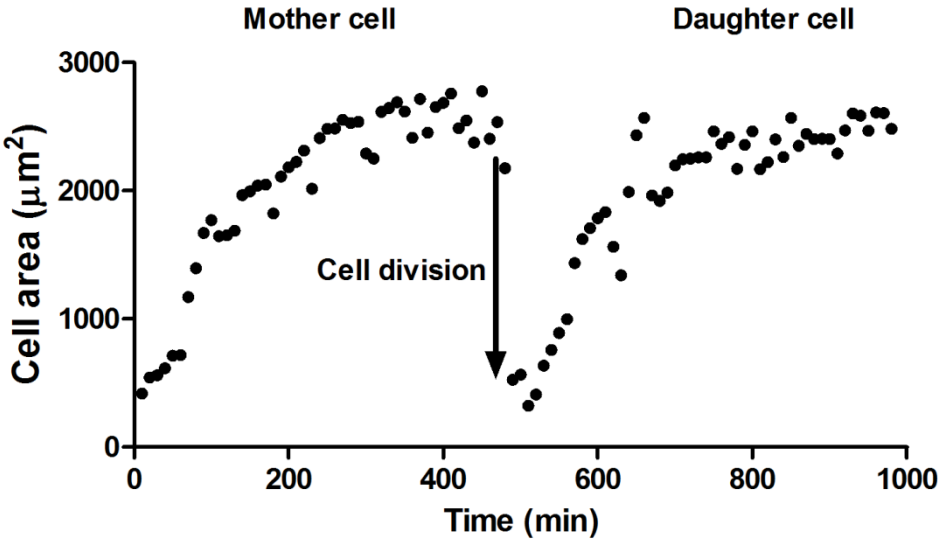

Figure S9. Changes of cell area during chemical and biological reattachment. NIH 3T3 cell was treated with trypsin to initiate reattachment. Cells show attachment by increasing in spreading area and after 400 minutes, cell division appears. The mother cell and daughter cell show identical cell spreading areas.

Video S1. **Reattachment process of cell from neonatal donor.** Cell was transfected with vimentin fluorescent plasmid and reattachment was initiated by treating cell with trypsin. Cell reattachment and migration was monitored for 18 h in 10 min intervals. Scale bar represent 20 μm.

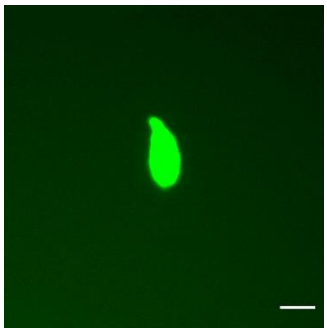

Video S2. **Reattachment process of cell from adult donor.** Cell was transfected with vimentin fluorescent plasmid and reattachment was initiated by treating cell with trypsin. Cell reattachment and migration was monitored for 20 h in 10 min intervals. Scale bar represent 20 μm.

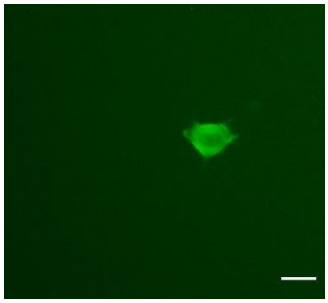

Video S3. **Cell division of NIH 3T3 during reattachment process.** Cell was transfected with actin-GFP plasmid and reattachment was initiated by treating cell with trypsin. Cell division process appears after cell is attached on the substrate. The full process of cell attachment and division was monitored for 16 h in 10 min intervals. Scale bar represent 20 μm.

Supplementary methods

Validation of cell reattachment. Trypsin treatment initiates a chemical reaction where proteins responsible for cell-matrix interaction are cleaved. We thus sought to verify that in our experiments trypsin had no detrimental effect on overall cell behavior and specifically that the trypsin-induced reattachment we monitored was comparable to a 'physiological' one such as when cells reattach after mitosis. For this, we used NIH 3T3 cell line, as it has a short doubling time and higher rates of transfection. NIH 3T3 cells at low density were transfected with actin-GFP and the reattachment experiment was initiated as described in the materials and methods section of the main manuscript. Cells successfully attached after trypsin treatment and some then underwent mitosis. Imaging of this subset of cells allowed us to compare the reattachment dynamics of trypsin-induced and mitosis-induced events (Movie S3). In particular, we quantified that changes in cell area for trypsin-induced reattachment displayed by the 'mother cell' were very similar to the mitosis-induced reattachment displayed by the 'daughter cell'. (Figure S9)